Vogiatzaki, K., Kronenburg, A., Cleary, M. J. & Kent, J. H. (2009). Multiple mapping conditioning of turbulent jet diffusion flames. Proceedings of the Combustion Institute, 32(2), pp. 1679-1685. doi: 10.1016/j.proci.2008.06.164



City Research Online

Original citation: Vogiatzaki, K., Kronenburg, A., Cleary, M. J. & Kent, J. H. (2009). Multiple mapping conditioning of turbulent jet diffusion flames. Proceedings of the Combustion Institute, 32(2), pp. 1679-1685. doi: 10.1016/j.proci.2008.06.164

Permanent City Research Online URL: http://openaccess.city.ac.uk/13366/

Copyright & reuse

City University London has developed City Research Online so that its users may access the research outputs of City University London's staff. Copyright © and Moral Rights for this paper are retained by the individual author(s) and/ or other copyright holders. All material in City Research Online is checked for eligibility for copyright before being made available in the live archive. URLs from City Research Online may be freely distributed and linked to from other web pages.

Versions of research

The version in City Research Online may differ from the final published version. Users are advised to check the Permanent City Research Online URL above for the status of the paper.

Enquiries

If you have any enquiries about any aspect of City Research Online, or if you wish to make contact with the author(s) of this paper, please email the team at publications@city.ac.uk.

Multiple Mapping Conditioning of turbulent jet diffusion flames

K. Vogiatzaki $^{\rm a},$ A. Kronenburg $^{\rm a,*},$ M.J. Cleary $^{\rm a-1}$, J.H. Kent $^{\rm b}$

 $^{\mathrm{a}}Department$ of Mechanical Engineering, Imperial College London, SW7 2AZ, U.K.

^bAerospace, Mechanical and Mechatronic Engineering, The University of Sydney,

Australia

Total length is 5317 words determined by method 2 for latex users

main text: 3568 references: 440

Figure 1: 132

Figure 2: 132

Figure 3: 143

Figure 4: 165

Figure 5: 209

Figure 6: 396 (two column figure)

Figure 7: 132

Email address: a.kronenburg@imperial.ac.uk (A. Kronenburg).

¹ Current address: Division of Mechanical Engineering, The University of Queensland, Australia

^{*} Corresponding author: A. Kronenburg, Dept. Mechanical Engineering, Imperial College London, Exhibition Rd., SW7 2AZ, UK

Abstract

The multiple mapping conditioning (MMC) approach is applied to two nonpiloted $CH_4/H_2/N_2$ turbulent jet diffusion flames with Reynolds numbers of Re=15,200 and Re=22,800. The work presented here examines primarily the suitability of MMC to simulate CH_4/H_2 flames with varying Re numbers. The equations are solved in a prescribed Gaussian reference space with only one stochastic reference variable emulating the fluctuations of mixture fraction. The mixture fraction is considered as the only major species on which the remaining minor species are conditioned. Fluctuations around the conditional means are ignored. It is shown that the statistics of the mapped reference field are an accurate model for the statistics of the physical field for both flames. A transformation of the Gaussian reference space introduced in previous work on MMC is used to express the MMC model in the same form as CMC. The most important advantage of this transformation is that the conditionally averaged scalar dissipation term is in a closed form. The corresponding temperature and reactive species predictions are generally in good agreement with experimental data. The application to real laboratory flames and the assessment of the new conditional scalar dissipation model for the closure of the singly conditioned CMC equation is the major novelty of this paper. The results are therefore primarily examined with respect to changes of the conditionally averaged quantities in mixture fraction space.

Key words: turbulent diffusion flame, modelling, scalar mixing, multiple mapping conditioning

1 Introduction

The primary focus of new model development in turbulent reacting flows is the accurate description of the coupling between reaction and molecular mixing and the associated closure problems for the terms representing these two processes. The closure of the chemical reaction rates is one of the most computationally challenging problems that arises. The non-linearities of the chemical reaction rates lead to terms involving correlations of the fluctuations that can be as large as those involving the average quantities. Consequently, attempts to express the average rates of reaction in terms of average values of the scalars have proved inadequate and species concentrations, which depend on reactions, cannot be predicted by unconditional averaging. Another important term is the turbulent mixing term. Bilger [1] showed that for the fast chemistry limit, reaction rates are strongly related to the scalar dissipation. Unfortunately, the dissipation appears as an unclosed term in most commonly used approaches.

The most recent advance in turbulent non-premixed combustion modelling is the Multiple Mapping Conditioning (MMC) method [2,3,4] that suggests a logical combination of Probability Density Function (PDF) [5,6] and Conditional Moment Closure (CMC) [7,8,9] approaches. The principle idea of MMC is the division of all turbulent fluctuations (and scalars) into "major" and "minor" groups. Fluctuations of major scalars are not restricted. Fluctuations of minor species are correlated to the fluctuations of major species and their evolution is determined by conditional methods.

MMC, as its name implies, employs the concept of the mapping closure (MC) [10,11,12]. Mapping functions map the quantities of interest (usually species

mass fraction) between a reference space with known distribution and the physical composition space whose distribution is unknown. The dimensionality of the reference space is determined by the number of major scalars. The chemical source terms are modeled with first-order moments and are conditioned on the reference variables. In the simplest formulation, the mixture fraction can be selected as the only major species and then MMC is equivalent to singly conditioned CMC but with the advantage that the conditional dissipation term appears in closed form. If all scalars in the composition space are selected as being major then MMC is equivalent to the joint PDF method. Therefore, it is clear that MMC is not a specific model, it is a generalised modelling approach. Depending on the actual implementation of the MMC principles, other models result as special cases of MMC.

The MMC model has been successfully tested in homogeneous, isotropic, decaying turbulence [13,14,15] and direct numerical simulation (DNS) has been used for validation. The current work deals with the extension to inhomogeneous laboratory flames. Mixture fraction is chosen as the only major species. The model is tested against experimental data for two non-piloted $CH_4/H_2/N_2$ flames studied at the Deutsches Zentrum fur Luft- und Raumfahrt (DLR) [16,17] and at Sandia Laboratories [18,19]. The two flames named as DLR A (Re=15,200) and DLR B (Re=22,800) are convenient for the present implementation since they have different Re numbers but at the same time neither presents considerable levels of local extinction and re-ignition. Predictions of doubly-conditioned MMC are necessary for flames with higher Re numbers, however, single conditioning will be sufficient for the present case since singly conditioned approaches have been proved successful in the past for flames with similar levels of extinction.

Despite the fact that DLR A and B are well characterised experimentally through extensive velocity and scalar measurements, only few modelling attempts have been performed. Pitsch [20] modelled the flame DLR A by combining a $k-\varepsilon$ model with an unsteady flamelet approach. Kempf et al. [21] applied a three dimensional Large Eddy Simulation (LES) for DLR A as well. Although the overall agreement of their results with experimental data is good, there is a clear tendency to radial diffusion close to the nozzle. More recently, Kim et al. [22] computed flame DLR B with a second order CMC for the reaction step, improving considerably NO predictions. Ozarovsky et al. [23] implemented a joint PDF approach closed at the joint scalar level for DLR A and DLR B and explored different methods of flame ignition. They also reported problems in predictions at the nozzle where steep gradients in mixture fraction necessitate accurate scalar dissipation estimates.

In the next section we introduce a deterministic MMC model with reference variable for mixture fraction. In Section 3, the numerical implementation is briefly described. Results for the mixture fraction are presented in Section 4. Finally, Section 5 focuses on the closure of the scalar dissipation term and its effect on the reactive species predictions.

2 The MMC model

The MMC equation given by [2]

$$\frac{\partial X_I}{\partial t} + \mathbf{U}\nabla X_I + A_k \frac{\partial X_I}{\partial \xi_k} - B_{kl} \frac{\partial^2 X_I}{\partial \xi_k \xi_l} = W_I \tag{1}$$

is solved in the reference space $\xi(\mathbf{x},t) = (\xi_1, \xi_2, ..., \xi_{major})$ for the mapping functions $\mathbf{X_I}$. The upper case subscript I stands for all scalars. The lower case

subscripts k and l are for the major scalars only. It is notable that a single equation governs the evolution of the mapping functions of all scalars of interest, without differentiating between major and minor groups. We emphasise that although the mapping functions simulate the evolution of the physical quantities of interest (i.e. species mass fraction), the reference field ξ does not represent by itself a direct model for any of the physical variables involved in combustion process. It is used only as a source of the stochastic behaviour of the modelling variables. It is noted here that the PDF of the reference field therefore can have an arbitrary shape, but previous work on mapping closure methods showed that a Gaussian reference space is mathematically convenient without limiting the generality of the method. The choice of the reference field however, affects the modelling of the parameters \mathbf{U} , A_k and B_{kl} that appear in Eq. (1) since models need to be consistent with the evolution equation of the reference PDF.

A standard Gaussian reference PDF, that is invariant in space and time, leads to a relatively simple form of the velocity, the drift and the diffusion coefficients, \mathbf{U} , A_k and B_{kl} . They are given by

$$\mathbf{U} = \mathbf{U}(\xi; \mathbf{x}, t) = \mathbf{U}^{(0)} + \mathbf{U}_k^{(1)} \xi_k$$
 (2)

$$A_k = -\frac{\partial B_{kl}}{\partial \xi_l} + B_{kl}\xi_l + \frac{1}{\overline{\rho}}\nabla \overline{\rho} \mathbf{U}_k^{(1)}$$
(3)

$$\mathbf{U}^{(0)} = \widetilde{\mathbf{v}} \tag{4}$$

$$\mathbf{U}_{k}^{(1)}\langle \xi_{k} X_{I} \rangle = \widetilde{\mathbf{v}' X_{I}'} \tag{5}$$

where $\bar{\rho}$ is the Reynolds average density, \mathbf{v} is the velocity vector, the tilde denotes Favre averages and angular brackets denote averages over reference space ξ .

The model proposed for the conditional velocity is linear (see Eq. (2)). It is based on a joint Gaussian distribution of the velocity and the scalar fields, and it is similar to the model commonly used in CMC computations. Joint Gaussianity is certainly questionable for velocity and mixture fraction, but it may hold for the joint distribution of velocity and the reference variable ξ_k .

For the Favre turbulent fluxes $\widetilde{\mathbf{v}'X_I'}$, the gradient diffusion hypothesis is applied.

$$\widetilde{\mathbf{v}'X_I'} = -D_t \langle \nabla X_I \rangle \tag{6}$$

The correlation $\langle \xi_k X_I \rangle$ is given by

$$\langle \xi_k X_I \rangle = \int \xi_k X_I P_{\xi_k} d\xi_k. \tag{7}$$

Eq. (2) to (5) imply that the diffusion coefficient can be treated as an independent coefficient. B_{kl} can be chosen as any reasonable function of (x, ξ) and then from Eq. (3) A_k can be determined so that a corresponding transport equation for the reference space PDF, P_{ξ} is satisfied [2]. However, from its interpretation as a diffusion coefficient which guarantees the consistency of the PDF of X_I with the joint species PDF transport equation, B_{kl} should satisfy the following relation [2]:

$$B_{kl} \left\langle \frac{\partial X_I \partial X_J}{\partial \xi_k \partial \xi_l} \right\rangle = \widetilde{N}_{IJ} \tag{8}$$

3 The MMC implementation

3.1 Case configuration

In the current study MMC is implemented for the modelling of two $CH_4/H_2/N_2$ turbulent jet diffusion flames (DLR A and DLR B). The fuel composition for both fuels is 22.1% CH_4 , 33.2% H_2 , and 44.7% N_2 by volume. The burner geometry features an axisymmetric fuel jet with diameter of 8mm and a surrounding nozzle with a dimeter of 140mm. The exit velocity of the cold jet is 42.2 ± 0.5 m/s for flame DLR A (Re = 15,200) and 63.2 ± 0.8 m/s for DLR B (Re = 22,800).

3.2 Numerical procedure

In the present study mixture fraction is chosen as the only major species and a standard Gaussian distribution of the reference variable is mapped to the mixture fraction field. The governing Eq. (1) then reduces to

$$\overline{\rho}\mathbf{U}\nabla X_Z + \overline{\rho}A\frac{\partial X_Z}{\partial \xi} - \overline{\rho}B\frac{\partial^2 X_Z}{\partial \xi^2} = 0$$
(9)

where ξ represents the one-dimensional reference space emulating mixture fraction X_Z . Time derivatives have been neglected due to the steady nature of the flow under investigation. The conservative form of Eq. (9) is:

$$\nabla \overline{\rho} \mathbf{U} X_Z + \overline{\rho} A \frac{\partial X_Z}{\partial \xi} - \overline{\rho} B \frac{\partial^2 X_Z}{\partial \xi^2} = X_Z \xi \nabla \overline{\rho} \mathbf{U}^{(1)}$$
(10)

Eq. (10) is discretised using a finite volume technique. The grid is staggered such that velocity is determined at the cell boundaries and scalars at the cell

centre. The computational domain extends to 100 diameters downstream and 19 diameters in radial direction and is discretised by 185 x 50 cells in the axial and radial directions, respectively. It is refined near the fuel port. For the reference variable ξ , 50 cells are used that cover the interval $\xi \in [-4,4]$.

A first-order upwinding scheme is used for spatial transport and a hybrid scheme is applied for discretising transport in ξ -space. This hybrid scheme changes from central differencing to first order upwind differencing when the Peclet number exceeds 2. Boundary conditions are defined in both physical and ξ -space. In the ξ -plane, the two boundary cells are calculated using the constant gradient assumption. The reader is referred to reference [24] for boundary conditions in physical space.

In the current implementation, Eq. (10) is solved for mixture fraction and coupled to an axisymmetric elliptic CFD code [24]. The solver uses the Biconjugate gradient method and produces results for all spatial and ξ -space locations at one time. Values for U, A, and B are computed explicitly, based on the solution of the previous iteration.

4 Mixture fraction modelling

The solution of Eq. (10) provides the evolution of mixture fraction in reference space if W_I is set to zero, and the mapping function represents mixture fraction, $Z = X_Z(\xi, x, r)$. The relationship between the reference PDF, the mapping function and the mixture fraction PDF, P_Z , is given by [11]

$$P_Z = P_{\xi} \left(\frac{\partial X_Z}{\partial \xi} \right)^{-1}. \tag{11}$$

The local mixture fraction mean and its rms can then easily be recovered by integration across reference space.

Figures 1 and 2 present the mean and the rms of Z as functions of radius at several downstream locations for flame DLR A and DLR B, respectively. It is shown that the predicted mean and variance of mixture fraction are in very good agreement with the experimental data for both flames. The variance is slightly under predicted further downstream. For better comparison, results from 'conventional' RANS computations for mean mixture fraction and rms are also included in these figures. The term 'conventional' refers to the solution of two transport equations for Favre averaged mixture fraction and its variance [25,26]. The quality of MMC and conventional RANS predictions is comparable and differences may be attributed to the different representation of the turbulent flux term. MMC predictions for the mean are better downstream than the corresponding RANS calculations. Both models predict the jet spreading reasonably well and are qualitatively similar to earlier RANS [23] and LES studies [21].

Figure 3 compares the predicted mixture fraction PDFs (solid lines) with the experimental data (squares) at three radial locations for x/D = 20. Further comparison is performed with the corresponding β -PDF profiles with mean and variance from the RANS calculations (dashed line). Agreement with experimental data is very good and predictions of MMC are improved in comparison to the β -PDF on the rich side (r/D < 1). The shapes of the two PDFs are very similar. It is well known that the β -PDF approximates the mixture fraction PDF very well and we may conclude that MMC leads to accurate predictions for the PDF. MMC does not, however, restrict the PDF shape and may therefore be useful in cases where we are interested in the joint PDF

of more than one scalar that cannot be easily presumed.

5 Chemical species predictions

A 35 species, 219 reaction mechanism has been employed [27] to simulate the chemical kinetics, and radiation losses were considered. In principle, Eq. (10) can be solved for all conditioning (here mixture fraction) and conditioned species (here all the reactive scalars). In the case of one reference variable however, a simple transformation [3,4] yields the singly conditioned moment closure (CMC) transport equations for the conditioned (reactive) species. The latter, i.e. the CMC equations, are solved here for convenience due to the existing CMC implementation in the code [24]. Conditional moment closure methods require closure of the mixture fraction PDF and of the conditional scalar dissipation rate. The current MMC implementation provides new closures for these terms, and the remainder of this paper will largely focus on scalar dissipation modelling and its effects on the reactive species predictions.

5.1 Scalar dissipation modelling

The MMC equation for the minor species is transformed using a coordinate transformation [3] from the Gaussian mixture fraction reference space, ξ , to the actual mixture fraction sample space variable η . Similar to Eq. (8), the conditional scalar dissipation can be obtained from

$$\langle N|\eta = Z(\xi)\rangle \approx B\left(\frac{\partial X_Z}{\partial \xi}\right)^2$$
 (12)

A simple integration of Eq. (12) over the reference space yields the mean scalar dissipation

$$\widetilde{N} = \int B \left(\frac{\partial X_Z}{\partial \xi}\right)^2 P_{\xi} d\xi \tag{13}$$

It is important to note that the mean scalar dissipation modelled as

$$\widetilde{N} = \frac{\varepsilon}{k} \widetilde{Z'^2},\tag{14}$$

links the turbulent flow field with the mixture fraction evolution and determines the diffusion coefficient B according to Eq. (8). The proposed MMC implementation provides a model for the conditional scalar dissipation and is fully closed. The modelling of the conditional scalar dissipation does not rely on pre-assumed PDFs for mixture fraction and is therefore distinctly different from existing closures [28,29].

Figure 4 compares the computed values of mean scalar dissipation obtained from MMC (solid lines) and conventional Favre averaged mixture fraction variance transport equations (dashed lines). General trends are similar for the two models, however, peak values are lower for the MMC model. The differences in unconditional dissipation are directly proportional to differences in variance predictions according to Eq. (14), and lower variances result in lower dissipation rates.

Figure 5 displays the radial profiles of conditional scalar dissipation at two downstream locations for flame DLR B. Solid lines represent the MMC predictions, the dash dotted lines show modelled dissipation values using an inverse error function as a shape function [30] and mean dissipation values that are based on the variance from the Favre averaged variance transport equation.

We will denote the latter model in the remainder of this paper 'error function model' (or erf). Not surprisingly, MMC yields lower predictions at all times due to lower mean dissipation rates. Some distinct differences can be observed with respect to the dissipation's distribution in mixture fraction space. The inverse error function gives always peak values at Z=0.5. This is certainly not correct at all times and locations, and MMC does not impose any restrictions on the shape of the conditionally averaged dissipation values. Indeed, the peak at x/D=5 varies with radial position. In addition, MMC predicts zero conditional scalar dissipation in zero probability regions as can be observed for high mixture fraction values at large radial positions.

5.2 Reactive scalar results

Figure 6 shows the conditional averages of temperature, CO and OH at three downstream locations and r/D=1 for flame DLR B. MMC predictions (solid lines) are compared with experiments (symbols) and a second set of CMC computations using a presumed β -PDF for mixture fraction and the 'error function model' for its conditional scalar dissipation (dashed dotted lines). It can be seen that the general behaviour is quite well reproduced for both models. The temperature is well predicted at all locations. For OH predictions, the MMC approach seems to offer considerably better predictions downstream (x/D=20 and further on). However, close to the nozzle it is overpredicted, which can probably be an indication of underprediction of scalar dissipation (cf. Fig. 5). In contrast, the CO predictions are somewhat lower than the experimental data for the MMC approach and the error function model seems to capture peak CO concentrations at x/D=20 and x/D=60 more accurately. However, if figure 6 is seen in conjunction with figure 2, it is clear that

in regions of high probability ($\eta = 0.3$ at x/D = 5, $\eta = 0.48$ at x/D = 20 and $\eta = 0.26$ at x/D = 60), MMC is qualitatively similar to the inverse error function model. We should also bear in mind, the relatively large measurement uncertainties of up to 25% for CO as reported in Meier et~al. [18].

The conditional profiles of major species such as CO_2 and H_2O are in good agreement with the experimental data for both flames. Differences between the predictions using different models of conditional scalar dissipation are quite small and results are therefore not shown.

Figure 7 shows radial profiles of unconditional temperature for DLR A and DLR B at three downstream locations. Good agreement is observed with the experimental data. The overprediction of temperature for radial locations with r/D > 1 at x/D = 5 can be associated with the early jet break up that is also noticeable in the mixture fraction profiles (Fig. 2). Generally, MMC leads to slightly improved temperature predictions, especially for flame DLR A, at x/D = 5 where the width of the high temperature region is less overpredicted in comparison to the error function model. The differences between the models reduce further downstream due to reduced differences in predicted values for conditional scalar dissipation.

6 Conclusion

The present work is the first deterministic application of the MMC approach to inhomogeneous reactive flows. For simplicity the MMC equation for only one major species has been solved and this major species represents mixture fraction. The MMC equation is solved with a Gaussian reference field and successful modelling for the PDF of the mapping function has been achieved.

It is demonstrated that the method is capable of simulating the structure of turbulent, non-piloted, diffusion flames with different levels of turbulence since trends for the first two moments of mixture fraction are very well reproduced.

MMC provides an implicit closure for the conditionally averaged scalar dissipation and the mixture fraction PDF which are needed for CMC, and MMC is therefore closed. These closures have been used for the prediction of reactive species and temperature and comparison with measurements shows good agreement and demonstrates the feasibility of this new method. Results are qualitatively similar to corresponding computations using more conventional closures based on transport equations for Favre averaged mixture fraction and its variance, but MMC provides a more consistent closure for the conditional dissipation, no assumptions on the shape of the PDF are required and its use may therefore be preferred in more complex geometries where standard assumptions on the shape of the PDF and the conditional dissipation may not hold. More detailed examination of the performance of the MMC model would require extra experimental data for the spatial profiles of the conditional scalar dissipation which are hoped to be available in the future.

The current study has demonstrated the feasibility of MMC to describe the evolution of the mixture fraction PDF. The suggested approach is, however, not limited to only one major scalar, and two or more major scalars will be needed for the accurate modelling of flames with moderate to significant local flame quenching. Modelling strategies for jet flames with extinction may be based on recent studies on scalar mixing in isotropic turbulence [15].

7 Acknowledgements

The authors acknowledge the financial support by EPSRC under grant number GR/T22766.

References

- [1] R.W. Bilger, Combust. Sci. Technol. 13 (1976) 155-170.
- [2] A.Y Klimenko, S.B. Pope, Phys. Fluids 15 (7) (2003) 1907-1925.
- [3] A.Y. Klimenko, Modern modelling of turbulent non-premixed combustion and reaction of pollution emission, Proceedings of Clean Air VII, Lisbon, Portugal, 2003.
- [4] A.Y. Klimenko, MMC modelling and fluctuations of the scalar dissipation, Australian Symposium on Combustion, Monash University, Melbourne, Australia, 2003.
- [5] S.B Pope, Prog. Energy Combust. Sci. 11 (1985) 119-192.
- [6] S.B. Pope, Advances in PDF Methods for Turbulent Reactive Flows, Proceedings of the Tenth Turbulence Conference, Barcelona, 2004.
- [7] A.Y. Klimenko, Fluid Dyn. 25 (1990) 327-334.
- [8] R.W. Bilger, Phys. Fluids A 5 (1993) 436-444.
- [9] A.Y. Klimenko, R.W. Bilger, Prog. Energy Combust. Sci. 25 (1999) 595-687.
- [10] H. Chen, S. Chen, R.H. Kraichnan, Phys. Rev. Lett. 63 (1989) 2657.
- [11] S.B Pope, Theoret. Comput. Fluid Dynamics 2 (1991) 255-270.
- [12] S.S. Girimaji, Phys. Fluids 4 (1992) 2875-2886.

- [13] A.P. Wandel, A.Y. Klimenko, Phys. Fluids 17 (12) (2005) 128105-1-128105-4.
- [14] M.J. Cleary, A. Kronenburg, Proc. Combust. Inst. 31 (2007) 1497-1505.
- [15] M.J. Cleary, A. Kronenburg, Combust. Flame 151 (4) (2007) 623-638.
- [16] W. Meier, S. Prucker, M.-H. Cao, W. Stricker, Combust. Sci. Technol. 118 (1996) 293-312.
- [17] W. Bergmann, W. Meier, D. Wolff, W. Stricker, Appl. Phys. B66 (1998) 489-502.
- [18] W. Meier, R.S. Barlow, Y.-L. Chen, J.-Y. Chen, Combust. Flame 123 (2000) 326-343.
- [19] C.H. Schneider, A. Dreizler, J. Janicka, E.P. Hassel, Combust. Flame 135 (2003) 185-190.
- [20] H. Pitsch, Combust. Flame 123 (2000) 358-374.
- [21] A. Kempf, C. Schneider, A. Sadiki, J. Janicka, Large Eddy Simulation of a Highly Turbulent Methane Flame: Application to the DLR Standard Flame, Proceeding of the 2nd Turbulent Shear Flow Phenomena (TSFP-II), 2001.
- [22] S.H. Kim, C.H. Choi, K.Y. Huh, Proc. Combust. Inst. 30 (2005) 735-742.
- [23] R.P. Lindstedt, H.C. Ozarovsky, Combust. Flame 143 (2005) 471-490.
- [24] M.J. Cleary, J.H. Kent, Combust. Flames 143 (4) (2005) 357-368.
- [25] J.H. Kent, R.W. Bilger, Proc. Combust. Inst. 14 (1973) 615-625.
- [26] W.P. Jones, B.E. Launder, International Journal of Heat and Mass Fraction 15 (1972) 301.
- [27] C.T. Bowman, R.K. Hanson, D.F. Davidson, J. Gardiner, W.C., V. Lissianski, G.P. Smith, D.M. Golden, M. Frenklach, M. Goldenberg, Gri-mech, available at http://www.me.berkeley.edu/gri-mech/.
- [28] S.S. Girimaji, Combust. Sci. Technol 107 (1995) 403-410.

- [29] C.B. Devaud, R.W. Bilger, T. Lui, $Phys.\ Fluids\ 16\ (2004)\ 2005-2011.$
- [30] N. Peters, $Prog.\ Energy\ Combust.\ Sci.\ 10\ (1984)\ 319-339.$

8 List of Figure Captions

Figure (1): Radial profiles of mixture fraction and mixture fraction rms at three axial locations for DLR A. Solid lines represent MMC predictions, dashed lines represent RANS and symbols represent experiments.

Figure (2): Radial profiles of mixture fraction and mixture fraction rms at three axial locations for DLR B. Solid lines represent MMC predictions, dashed lines represent RANS and symbols represent experiments.

Figure (3): PDF profiles of mixture fraction at x/D = 20. Squares represent experimental data, solid lines represent MMC predictions and dashed lines β -PDF.

Figure (4): Radial profiles of mean scalar dissipation at three axial location for DLR B. Solid lines represent MMC predictions and dashed lines represent predictions from conventional Favre averaged mixture fraction variance transport equation.

Figure (5): Conditional scalar dissipation at x/D = 5 (left) and x/D = 20 (right) for various radial positions in flame DLR B. Solid lines represent MMC predictions and dashed dotted lines inverse error function.

Figure (6): Conditional profiles of T, CO and OH at r/D = 1 at three down-stream locations. Squares represent experimental data, solid lines represent MMC predictions and dashed dotted lines CMC predictions with the inverse error function model for the conditional scalar dissipation.

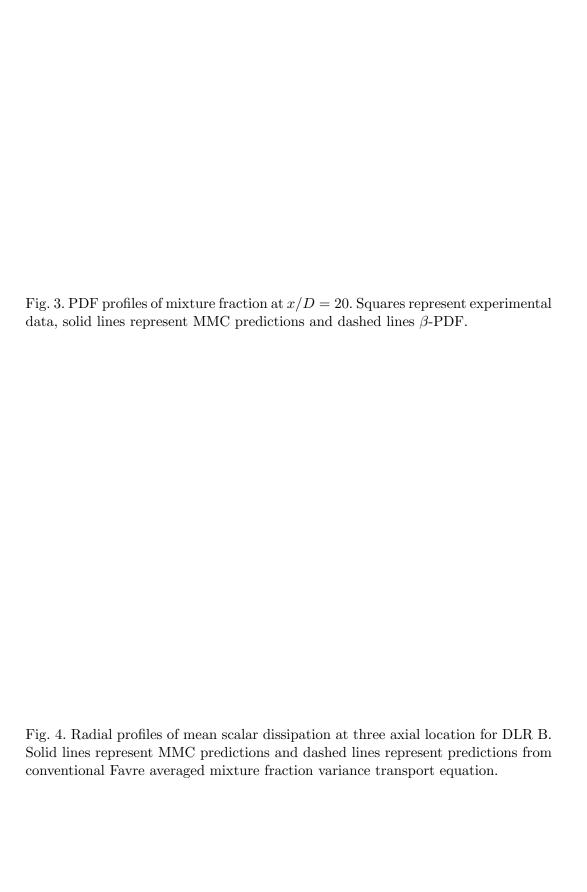
Figure (7): Radial profiles of temperature at three axial locations for DLR A and DLR B. Solid lines represent MMC predictions, dashed dotted lines CMC

predictions with the inverse error function model for the conditional scalar dissipation and symbols represent experiments.



Fig. 1. Radial profiles of mixture fraction and mixture fraction rms at three axial locations for DLR A. Solid lines represent MMC predictions, dashed lines represent RANS and symbols represent experiments.

Fig. 2. Radial profiles of mixture fraction and mixture fraction rms at three axial locations for DLR B. Solid lines represent MMC predictions, dashed lines represent RANS and symbols represent experiments.



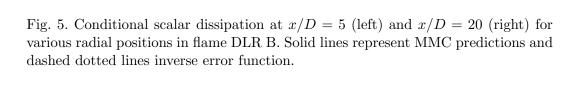


Fig. 6. Conditional profiles of T, CO and OH at r/D=1 at three downstream locations for DLR B. Solid lines represent MMC predictions and dashed dotted lines CMC predictions with the inverse error function model for the conditional scalar dissipation.

Fig. 7. Radial profiles of temperature at three axial locations for DLR A and DLR B.Solid lines represent MMC predictions, dashed dotted lines CMC predictions with the inverse error function model for the conditional scalar dissipation and symbols represent experiments.